

Robust Monitoring of Time Series with Application to Fraud Detection

Peter Rousseeuw, Domenico Perrotta, Marco Riani and Mia Hubert

December 14, 2024

Abstract

Time series often contain outliers and level shifts or structural changes. These unexpected events are of the utmost importance in fraud detection, as they may pinpoint suspicious transactions. The presence of such unusual events can easily mislead conventional time series analysis and yield erroneous conclusions. In this paper we provide a unified framework for detecting outliers and level shifts in short time series that may have a seasonal pattern. The approach combines ideas from the FastLTS algorithm for robust regression with alternating least squares. The double wedge plot is proposed, a graphical display which indicates outliers and potential level shifts. The methodology was developed to detect potential fraud cases in time series of imports into the European Union, and is illustrated on two such series.

Keywords: alternating least squares, double wedge plot, level shift, outliers.

Peter Rousseeuw, Department of Mathematics, University of Leuven, Belgium. Domenico Perrotta, Joint Research Centre, Ispra, Italy. Marco Riani, Department of Economics, University of Parma, Italy. Mia Hubert, Department of Mathematics, University of Leuven, Belgium. Peter Rousseeuw and Mia Hubert gratefully acknowledge the support by project C16/15/068 of Internal Funds KU Leuven. The work of Domenico Perrotta was supported by the Project “Automated Monitoring Tool on External Trade Step 5” of the Joint Research Centre and the European Anti-Fraud Office of the European Commission, under the Hercule-III EU programme. In this paper, references to specific countries and products are made only for purposes of illustration and do not necessarily refer to cases investigated or under investigation by anti-fraud authorities.

1 Introduction

When analyzing time series one often encounters unusual events such as outliers and structural changes, like those in Figure 1. Both series track trade volumes, and were extracted from the official trade statistics in the COMEXT database of Eurostat. This database contains monthly trade volumes (aggregated over several transactions, possibly involving different traders) of products imported in the European Union (EU) in a four-year period. The plot titles in Figure 1 specify the code of the traded product in the EU Combined Nomenclature classification (CN code), the country of origin, and the destination (a member state of the EU). The CN code determines whether the volumes are expressed in tons of net mass and/or other units (liters, number of items, etc.), the rate of customs duty applied, and how the goods are treated for statistical purposes. The data quality is quite heterogeneous across countries and products, but some macroscopic outliers (manifest errors) have already been removed or corrected by statistical authorities and customs services.

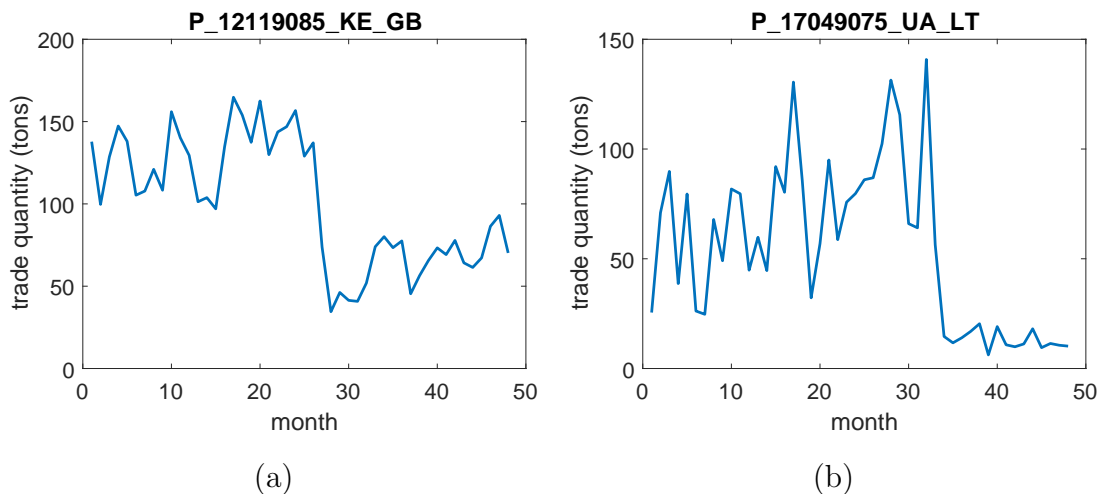


Figure 1: Monthly trade volumes of two products imported in the European Union in a four-year period: (a) imports of plants used primarily in perfumery, pharmacy or for insecticidal, fungicidal or similar purposes, from Kenya into the UK (P12119085-KE-GB); (b) import of sugars including chemically pure lactose, maltose, glucose and fructose, sugar syrups, artificial honey and caramel, from the Ukraine into Lithuania (P17049075-UA-LT).

Both of these time series exhibit a downward level shift. Knowing when such structural

breaks occur is important for fraud detection. For instance, a sudden reduction in trade volume may coincide with an increase for a related product or another country of origin, which could indicate a misdeclaration with the intent of deflecting customs duties.

There are many products and countries of origin in the CN classification, but not all of these combinations occur and the number of products at risk of fraud is relatively small. Still, the number of relevant combinations of a product at fraud risk, a country of origin and a country of destination is around 16,000. As a result, every month around 16,000 time series need to be analyzed for anti-fraud purposes. This requires an automatic approach that is able to report accurate information on outliers and the positions and amplitudes of level shifts, and that runs fast enough for that time frame. The method proposed in this paper meets those objectives, and provides a graphical display that can be looked at whenever the automatic monitoring system detects a significant level shift.

A different statistical approach to monitor international trade data for fraud was proposed by Barabesi et al. (2016) who tested whether the distribution of trade volumes follows the Newcomb-Benford law. In the current paper we also take the time sequence of the trades into account. We will focus on a parametric approach to estimate level shifts, which differs from the nonparametric smoothing methods in Fried and Gather (2007) or robust methods for REGARIMA models (Bianco et al., 2001). See also Galeano and Peña (2013) for a review of robust modeling of linear and nonlinear time series.

The structure of the paper is as follows. In Section 2 we introduce our model and methodology for robustly analyzing a time series which contains a trend, a seasonal component and possibly a level shift in an unknown position, as well as isolated or consecutive outliers. In Section 3 we illustrate the proposed approach using the well-known airline data (Box and Jenkins, 1976), as well as contaminated versions of it in order to test the ability of the method to detect anomalies. In this section we also introduce the double wedge plot, which visualizes the presence of a level shift and outliers. In Section 4 we apply our methodology to the time series in Figure 1 and compare the analysis with that obtained by a nonparametric method. Section 5 concludes, and the Appendix proves a result about our algorithm.

2 Methodology

2.1 The model

The time series $y(t) = y_t$ (for $t = 1, \dots, T$) we will consider may contain the following terms:

1. a polynomial trend, i.e. $\sum_{a=0}^A \alpha_a t^a$;
2. a seasonal component, i.e.

$$S_t = \sum_{b=1}^B \left(\beta_{b,1} \cos \left(\frac{2\pi b}{12} t \right) + \beta_{b,2} \sin \left(\frac{2\pi b}{12} t \right) \right) . \quad (1)$$

When $B = 1$ this is periodic with a one-year period, $B = 2$ corresponds with a six-month period etc. We assume the amplitude of the seasonal component varies over time in a polynomial way, i.e. $y_t \sim \left(1 + \sum_{g=1}^G \gamma_g t^g \right) S_t$;

3. a level shift in an unknown time point $2 \leq \delta_2 \leq T$, i.e. $\delta_1 I(t \geq \delta_2)$ with $I(\cdot)$ the indicator function.

The general model is thus of the form

$$y_t = \sum_{a=0}^A \alpha_a t^a + \left[\sum_{b=1}^B \left(\beta_{b,1} \cos \left(\frac{2\pi b}{12} t \right) + \beta_{b,2} \sin \left(\frac{2\pi b}{12} t \right) \right) \right] \left(1 + \sum_{g=1}^G \gamma_g t^g \right) + \delta_1 I(t \geq \delta_2) + \varepsilon_t \quad (2)$$

where ideally the errors ε_t are i.i.d. and normally distributed. Let us collect all unknown parameters in a vector $\theta = (\alpha_0, \alpha_1, \dots, \beta_{1,1}, \beta_{1,2}, \dots, \gamma_1, \gamma_2, \dots, \delta_1, \delta_2)$ of length p . Then model (2) can be written as

$$y_t = f(\theta, t) + \varepsilon_t$$

with $f(\theta, t) = \sum_{a=0}^A \alpha_a t^a + S_t(1 + \sum_{g=1}^G \gamma_g t^g) + \delta_1 I(t \geq \delta_2)$ and $\varepsilon_t \sim N(0, \sigma^2)$. The time series does not need to contain all of these components, as some coefficients can be zero.

2.2 The nonlinear LTS estimator

Model (2) is nonlinear in the parameters $\beta_{b,1}$, $\beta_{b,2}$, γ_g and δ_2 . As there may be outliers in the time series, we propose to estimate θ by means of the *nonlinear least trimmed squares*

(NLTS) estimator (Rousseeuw, 1984; Stromberg and Ruppert, 1992; Stromberg, 1993):

$$\hat{\theta}_{\text{NLTS}} = \underset{\theta}{\operatorname{argmin}} \sum_{j=1}^h r_{(j)}^2(\theta) \quad (3)$$

where $T/2 \leq h < T$ and $r_{(j)}^2(\theta)$ is the j -th smallest squared residual $(y_t - f(\theta, t))^2$. Our default choice for h is $[0.75n]$.

The \sqrt{n} -consistency and asymptotic normality of NLTS were studied by Čížek (2005, 2008). To compute the estimator, we propose to combine ideas from the FastLTS algorithm for robust linear regression (Rousseeuw and Van Driessen, 2006) with the alternating least squares (ALS) method.

We first describe how we use the alternating least squares procedure. We temporarily assume that the estimated shift time $\hat{\delta}_2$ is fixed, and that we want to solve (3) for a subset of the y_t with at least $p - 1$ observations, at least one of which is to the left of $\hat{\delta}_2$ and at least one of which is equal or to the right of $\hat{\delta}_2$. We denote the indices of the subset as $E \subset \{1, 2, \dots, T\}$ with $\#E \geq p - 1$, where E must overlap with $\{1, \dots, \hat{\delta}_2 - 1\}$ as well as $\{\hat{\delta}_2, \dots, T\}$. These conditions are required to make the parameters in (2) identifiable from the subset $y_E = \{y_t; t \in E\}$. We then go through the following steps:

1. **[Initialization]** Set $\gamma_g = 0$ for $g = 1, \dots, G$. Then a part of (2) drops out, leaving

$$y_t = \sum_{a=0}^A \alpha_a t^a + \sum_{b=1}^B \left(\beta_{b,1} \cos\left(\frac{2\pi b}{12}t\right) + \beta_{b,2} \sin\left(\frac{2\pi b}{12}t\right) \right) + \delta_1 I(t \geq \hat{\delta}_2) + \varepsilon_t \quad (4)$$

which is linear in the parameters α_a , $\beta_{b,1}$, $\beta_{b,2}$ and δ_1 . By applying linear LS to the entire data set $\{y_t; t = 1, \dots, T\}$ we obtain the estimates $\hat{\alpha}_a^{(0)}$, $\hat{\beta}_{b,1}^{(0)}$, $\hat{\beta}_{b,2}^{(0)}$ and $\hat{\delta}_1^{(0)}$.

2. **[Iteration]** For $k = 1, 2, \dots$ repeat the following steps:

- **[ALS step A]** Let $S_t^{(k-1)} = \sum_{b=1}^B \left(\hat{\beta}_{b,1}^{(k-1)} \cos\left(\frac{2\pi b}{12}t\right) + \hat{\beta}_{b,2}^{(k-1)} \sin\left(\frac{2\pi b}{12}t\right) \right)$ in which the coefficients $\hat{\beta}_{b,1}^{(k-1)}$ and $\hat{\beta}_{b,2}^{(k-1)}$ come from the previous step. Keeping $S_t^{(k-1)}$ fixed yields the model

$$y_t - S_t^{(k-1)} = \sum_{a=0}^A \alpha_a t^a + S_t^{(k-1)} \left(\sum_{g=1}^G \gamma_g t^g \right) + \delta_1 I(t \geq \hat{\delta}_2) + \varepsilon_t \quad (5)$$

which is linear in the parameters α_a , γ_g , and δ_1 . We then apply LS using only the observations in the subset y_E , yielding the estimates $\hat{\alpha}_a^{(k)}$, $\hat{\gamma}_g^{(k)}$ and $\hat{\delta}_1^{(k)}$.

- **[ALS step B]** Keeping the estimated coefficients $\hat{\alpha}_a^{(k)}$, $\hat{\gamma}_g^{(k)}$ and $\hat{\delta}_1^{(k)}$ from the previous step fixed yields the model

$$y_t - \sum_{a=0}^A \alpha_a^{(k)} t^a - \hat{\delta}_1^{(k)} I(t \geq \hat{\delta}_2) = \left[\sum_{b=1}^B \left(\beta_{b,1} \cos\left(\frac{2\pi b}{12}t\right) + \beta_{b,2} \sin\left(\frac{2\pi b}{12}t\right) \right) \right] \left(1 + \sum_{g=1}^G \hat{\gamma}_g^{(k)} t^g \right) + \varepsilon_t \quad (6)$$

which is linear in the parameters $\beta_{b,1}$ and $\beta_{b,2}$. We then apply LS using only the observations in the subset y_E , yielding the estimates $\hat{\beta}_{b,1}^{(k)}$ and $\hat{\beta}_{b,2}^{(k)}$. Then we go back to ALS step A.

Let $\hat{\theta}_k$ be the vector of coefficients after iteration step k . We repeat the above steps until $\|\hat{\theta}_k - \hat{\theta}_{k-1}\|/\|\hat{\theta}_{k-1}\|$ is below a threshold, or a maximal number of iterations (say 50) is attained.

In words, ALS solves the nonlinear LS problem of fitting (2) to the data set y_E by alternating between the solution of two linear LS fits, (5) and (6).

Our goal is to solve the nonlinear LTS problem (3). A basic tool for linear LTS is the **C-step** (Rousseeuw and Van Driessen, 2006) which we now generalize to the nonlinear setting. Given an initial fit $\hat{\theta}^{(0)}$ obtained by applying ALS to a subset of the y_t , we compute the residuals $r_t = y_t - f(\hat{\theta}^{(0)}, t)$ for the whole time series (that is, for $t = 1, \dots, T$) and retain the h observations with smallest squared residuals. To this new subset we apply ALS again, yielding a new fit. It is shown in the Appendix that the new fit is guaranteed to have a lower objective function. It is possible to iterate the C-step until convergence, which will occur in a finite number of steps.

Using these building blocks, we now describe the entire algorithm to compute the NLTS fit to the model (2). Let $t_{(1)}, \dots, t_{(S)}$ be the ordered indices of the possible positions δ_2 of the level shift, for example the set $\{u+1, \dots, T-u\}$ for some $u > 0$. The algorithm then consists of the following steps.

1. **Find best solutions for $t_{(s)}$ where $s = 1, \dots, S$.** We temporarily set $\hat{\delta}_2 = t_{(s)}$.
 - (a) Run the above initialization step, yielding initial coefficients.
 - (b) For m ranging from 1 to the number of subsets M ,

- i. Construct an elemental subset E containing $p - 1$ different observations. This subset should contain the index $t_{(s)}$, one observation y_t with $t < t_{(s)}$ and $p - 3$ observations drawn at random from the whole time series.
- ii. Apply ALS-steps (always keeping $\hat{\delta}_2 = t_{(s)}$ fixed), followed by two C-steps. If a singular solution is obtained during the computations, restart without increasing m .

In our experiments we found that $M = 250$ was sufficient to guarantee stable results.

- (c) Consider only the *nbest* elemental subsets that yielded the lowest objective function so far. Apply C-steps to them until full convergence and store the values of the *nbest* solutions. In our examples we found that setting *nbest* to 10 worked well.
- (d) If $s > 1$ also apply C-steps until convergence starting from the *nbest* best elemental sets from step $s - 1$, but using the new position $\hat{\delta}_2 = t_{(s)}$.
- (e) Take the fit with the lowest objective among these $2nbest$ candidates, and denote it by $\hat{\theta}^{(s)}$.
- (f) Store the corresponding scaled residuals

$$\tilde{r}_t(\hat{\theta}^{(s)}) = \frac{r_t(\hat{\theta}^{(s)})}{\sqrt{\sum_{t=1}^h r_{(t)}^2(\hat{\theta}^{(s)})/h}} \quad \text{for } t = 1, \dots, T. \quad (7)$$

2. **Retain overall best solution.** Among the fits $\hat{\theta}^{(s)}$ for $s = 1, \dots, S$ take the one with lowest objective function $\sum_{t=1}^h r_{(t)}^2(\hat{\theta}^{(s)})$ and denote it by $\hat{\theta}^{opt}$.

For estimating the scale of the error term we can use $\sum_{t=1}^h r_{(t)}^2(\hat{\theta}^{opt})$. But since this sum of squares only uses the h most central residuals, the estimate needs to be rescaled. The variance of a truncated normal distribution containing the central h/n portion of the standard normal is

$$\sigma_{Tr}^2(h) = 1 - \frac{2n}{h} \Phi^{-1} \left(\frac{n+h}{2n} \right) \phi \left\{ \Phi^{-1} \left(\frac{n+h}{2n} \right) \right\}$$

by equation (6.5) in (Croux and Rousseeuw, 1992). Therefore we compute

$$\tilde{\sigma}^2 = \sum_{t=1}^h r_{(t)}^2(\hat{\theta}^{opt}) / (h \sigma_{Tr}^2(h)). \quad (8)$$

Note that this makes $\tilde{\sigma}^2$ consistent, but not yet unbiased for small samples. Therefore we include the finite-sample correction factor from Pison et al. (2002) in our final scale estimate $\hat{\sigma}$.

3. **Locally improving the shift position estimate.** The previous steps have yielded an estimate $\hat{\delta}_2$ of the position of the level shift, but it may be imprecise. For instance, it may happen that the h -subset underlying $\hat{\theta}^{opt}$ does not itself contain the time points $\hat{\delta}_2$ or $\hat{\delta}_2 + 1$. In order to improve the estimate we check in its vicinity as follows:

- Take a window W around $\hat{\delta}_2$. For each t^* in W , we replace $\hat{\delta}_2$ by t^* while keeping the other coefficients from $\hat{\theta}^{(opt)}$ and the scale estimate $\hat{\sigma}$. Compute the residuals r_t from these coefficients and let $f(t^*) = \sum_{t \in W} \rho(r_t/\hat{\sigma})$ with ρ the Huber function

$$\rho(x) = \begin{cases} x^2/2 & \text{if } |x| \leq b \\ b|x| - b^2/2 & \text{if } |x| > b \end{cases}$$

In our simulations and the analysis of international trade time series (of the kind given in Figure 1) the best results were obtained with b equal to 1.5 or 2. In our implementation the defaults are $b = 2$ and a window W of width 15.

- Our final $\hat{\delta}_2$ is the t^* in W with lowest $f(t^*)$. If it is different from the estimate we had before, we recompute the scaled residuals.
4. **Weighted step.** We apply the univariate outlier detection procedure described in (Gervini and Yohai, 2002) and (Agostinelli et al., 2015) to the T scaled residuals $(y_t - f(\hat{\theta}^{(opt)}, t))/\hat{\sigma}$. By default we use the 99% confidence level. Alternatively, one could use the thresholds obtained in Salini et al. (2015).
 5. **Final fit.** We apply nonlinear LS to all the points that have not been flagged as outliers in the previous step, starting from the initial estimate $\hat{\theta}^{(opt)}$ and keeping $\hat{\delta}_2$ fixed. For this we can iterate ALS steps until convergence. The standard errors obtained in the last two ALS steps can be used for inference.

The Matlab code of the algorithm can be downloaded from [/www.riani.it/rprh/](http://www.riani.it/rprh/). In the following sections we will apply it to several data sets.

3 Airline data and the double wedge plot

The airline passenger data, given as Series G in Box and Jenkins (1976), has often been used in the time series analysis literature as an example of a nonstationary seasonal time series. It consists of $T = 144$ monthly total numbers of airline passengers from January 1949 to December 1960. Box and Jenkins developed a two-coefficient time series model of factored form that is now known as the airline model. In this section we will analyze these data using our method, and then contaminate the data in various ways to see how the method reacts.

Uncontaminated data. We fit the data by model (2) with $A = 2$, $B = 4$ and $G = 2$. This means that we assume a quadratic trend, a quarterly seasonal component, and a quadratically varying amplitude. The resulting NLTS fit (3) closely follows the data, as can be seen in Figure 2. In this example no data point has been flagged as outlying. From the standard errors (not shown) we conclude that all coefficients are significant except for the height of the level shift.

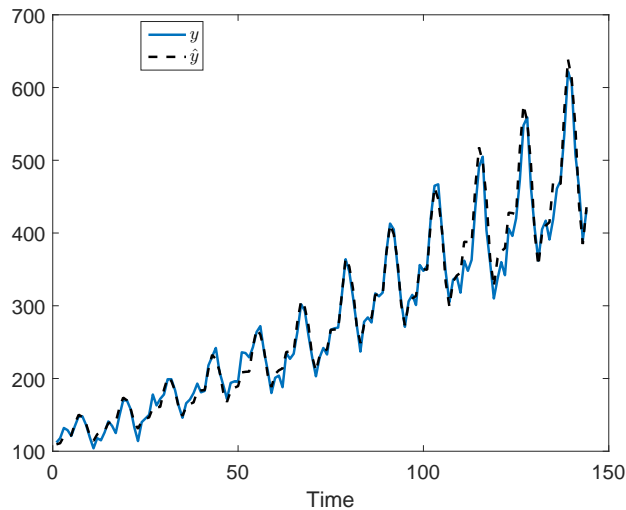


Figure 2: Airline data: observed and fitted values based on model (2) with a quadratic trend, a quarterly seasonal component, and a quadratically varying amplitude.

Contamination 1. We now contaminate the series by adding two groups of outliers in opposite directions and one isolated outlier, yielding the blue curve in the bottom panel of Figure 3. More precisely, the value 300 is subtracted from all responses in the interval

$[50, 55]$ while 300 is added on $[70, 75]$ and at $t = 90$. The fitted values (dotted curve) from NLTS closely follow the observed values for the regular observations. The flagged outliers are indicated by red crosses, whose size is proportional to the absolute magnitude of their residual. We see that all the outliers we added are clearly recognized as such, and they were not used to estimate the coefficients in the weighted step. Only a few regular observations received an absolute residual slightly above the cutoff value.

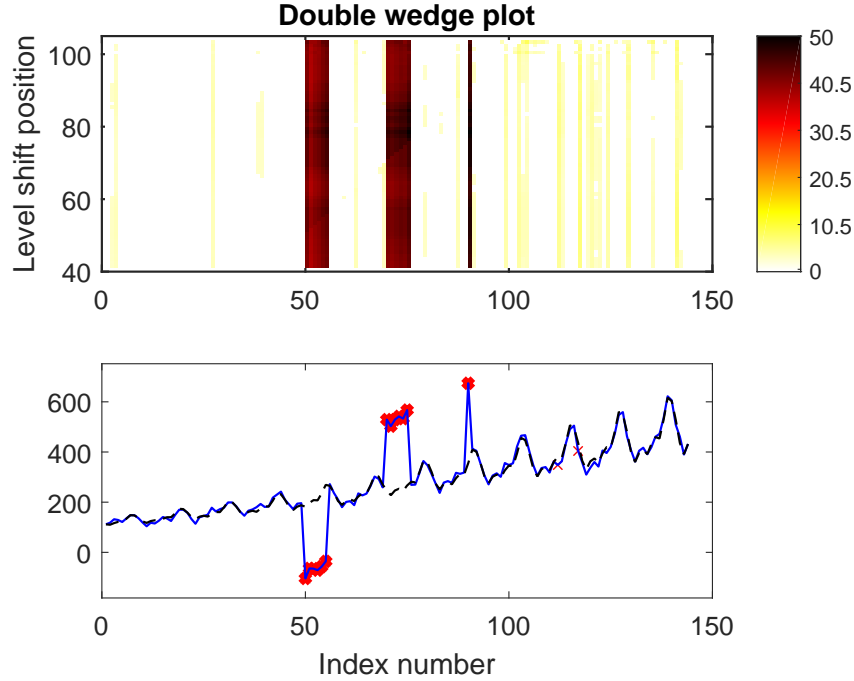


Figure 3: Airline data with contamination 1: double wedge plot (top) and observed and fitted values (bottom).

The top panel of Figure 3 is a byproduct of the algorithm, and is useful for visualizing the presence of (groups of) outliers and a level shift. The first step of the algorithm ranges over all potential positions $t_{(1)}, \dots, t_{(S)}$ of a level shift. These tentative positions $t_{(s)}$ are on the vertical axis. (Here we took $t_{(1)} = 40$ and $t_{(S)} = 103$.) For any $t_{(s)}$ we plot the absolute scaled residuals $|\tilde{r}_t(\hat{\theta}^{(s)})|$ given in (7), in all of the times $t = 1, 2, \dots, T$ on the horizontal axis. The color in the plot depends on the size of that absolute residual and ranges from black (large residuals) over red and yellow to white (small residuals). The color scale is at the right of the plot. Scaled residuals larger than 50 are shown as if they were 50, so that even a very far outlier cannot affect the color coding. In the same spirit, uninformative

scaled residuals smaller than 2.5 are shown as if they were 0, so in white. Of course the user can easily modify these default choices.

Outliers have a large absolute scaled residual from the robust fit, so in this plot isolated outliers will appear as dark vertical lines, and groups of consecutive outliers as dark vertical bands. In this example we clearly see the contamination. The regular observations with scaled residual slightly above 2.5 do not stand out as they are in light yellow.

Contamination 2. In the second contamination setting we introduce a persistent level shift and three isolated outliers, two of which lie in the proximity of the level shift which makes the problem harder. For this we added the value 1300 to all responses from $t = 68$ onward, at $t = 45$ the response is lowered by 800, at $t = 67$ by 600, while at $t = 68$ and $t = 69$ we added an additional 800.

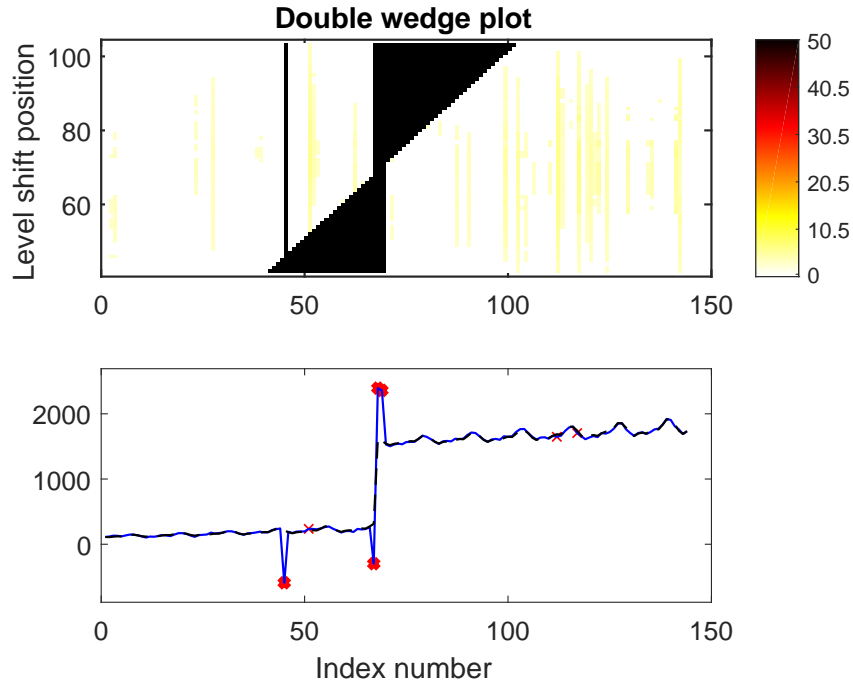


Figure 4: Airline data with contamination 2.

The bottom panel of Figure 4 shows the observed and fitted values. Again all inserted outliers are clearly detected, and a few regular observations have small crosses indicating that their scaled absolute residual was slightly above 2.5.

The plot of the absolute scaled residuals $|\tilde{r}_t(\hat{\theta}^{(s)})|$ in the top panel of Figure 4 now looks more eventful with two dark triangles. Together these ‘wedges’ signal a level shift.

To understand this effect, let us assume that the true level shift is at position t^* and the algorithm is in the process of checking the candidate $t_{(s)} = t^* - r$. Then the algorithm will treat the y_t at $t^* - r + 1, \dots, t^* - 1$ as outliers and the resulting robust fit (still for that $t_{(s)}$) will show $r - 1$ consecutive outliers. Similarly, when the algorithm tries $t_{(s)} = t^* + r$ to the right of t^* , the best solutions will show r outliers. As a result, when approaching the true level shift position t^* from the left the scaled residuals we are monitoring will form a dark upward-pointing wedge, and to the right of the true t^* we obtain an analogous wedge pointing downward. In the top panel of Figure 4, we observe two opposite wedges tapering off in the proximity of the true level shift position, around $t = 68$. In this region we observe a small rectangle (centered at position 68) bridging the two wedges. The rectangle is due to the two outliers in the proximity of the level shift. The isolated outlier at position 45 yields a single dark vertical line like those in Figure 3.

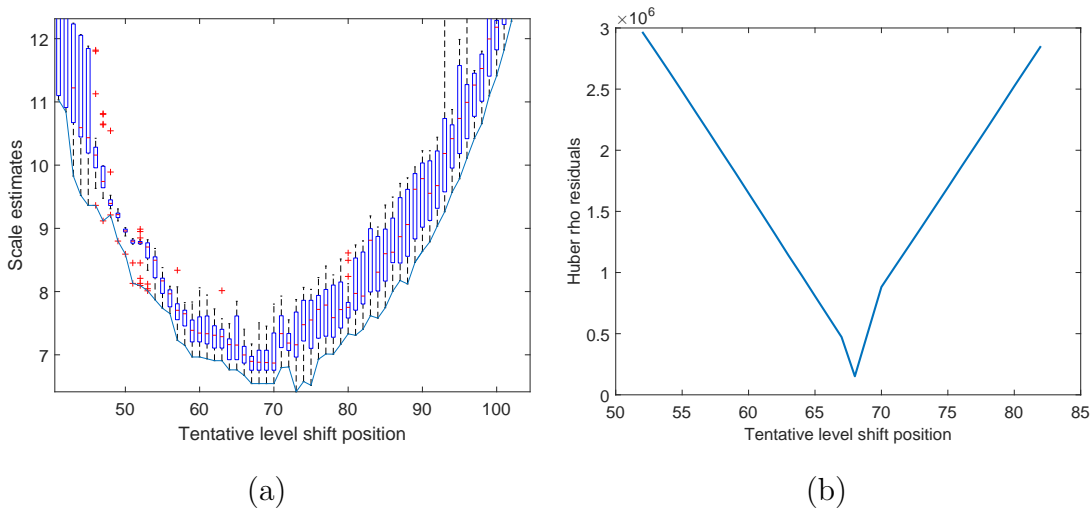


Figure 5: Airline data with contamination 2: (a) boxplots of the 20 lowest objective function values attained at each $t_{(s)}$; (b) local improvement of the shift position estimate.

Panel (a) of Figure 5 shows the boxplots of the objective function $\sum_{t=1}^h r_{(t)}^2(\hat{\theta}_j^{(s)})$ attained by the $2nbest = 20$ best solutions $\hat{\theta}_j$ in step 1(e) of the algorithm. It is thus also a free byproduct of the estimation. If a level shift is present in the central part of the time series, this plot will typically have a U shape. In this example the lowest values of the trimmed sum of squared residuals occur in the time range 60-80. The continuous curve which connects the lowest objective value for each s reaches its global minimum at $t_{(s)} = 73$. However,

the curve is quite bumpy in that region, with several local minima and a near-constant stretch on 67-70, so the position of the minimum is not precise. This kind of situations motivated the local improvement in step 3 of the algorithm. Panel (b) of Figure 5 shows $f(t_{(s)}) = \sum_{t \in W} \rho(r_t/\hat{\sigma})$ as a function of the tentative position $t_{(s)}$ (with ρ the Huber function with $b = 2$) on the interval 53-82. This curve has a much better determined minimum, in fact at $t = 68$, confirming the benefit of the local improvement step.

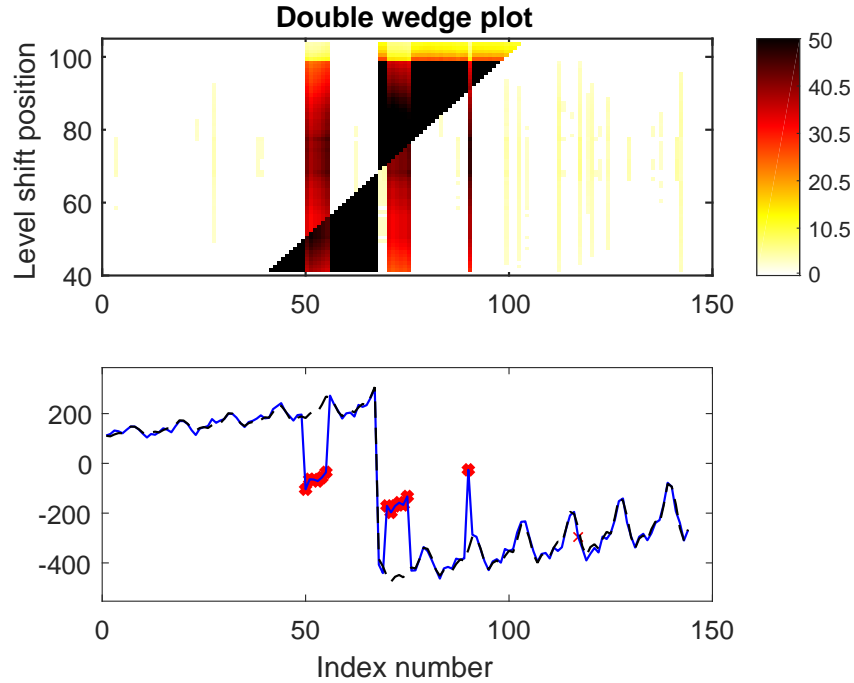


Figure 6: Airline data with contamination 3.

Contamination 3. In the final contaminated dataset we inserted a level shift and a group of consecutive outliers following it. To complicate things even more, we also put in a stretch of contamination to the left of the level shift, as well as an isolated outlier. The bottom panel of Figure 6 shows the robust fit, which succeeded in recovering the structure and flagging the outliers. In the top panel of Figure 6 we see the typical double wedge pattern indicating a level shift. The two reddish bands flag the groups of consecutive outliers, whereas the single line corresponds to the isolated outlier at $t = 90$. In this example the thick end of the upper wedge is yellow, so the absolute scaled residuals are not as large there. This part corresponds to a tentative level shift of around 100, which is very far from the true one, and in such cases the fit may indeed be quite different.

4 Analysis of trade data

Our main goal is to analyze the many short time series of trade described in Section 1. After trying several model specifications in the class (2) we found that the best results were obtained by using a linear trend, two harmonics, and one parameter to model the varying amplitude of the seasonal component, that is, $A = 1$, $B = 2$ and $G = 1$. As an example we now apply our method to the time series in Figure 1.

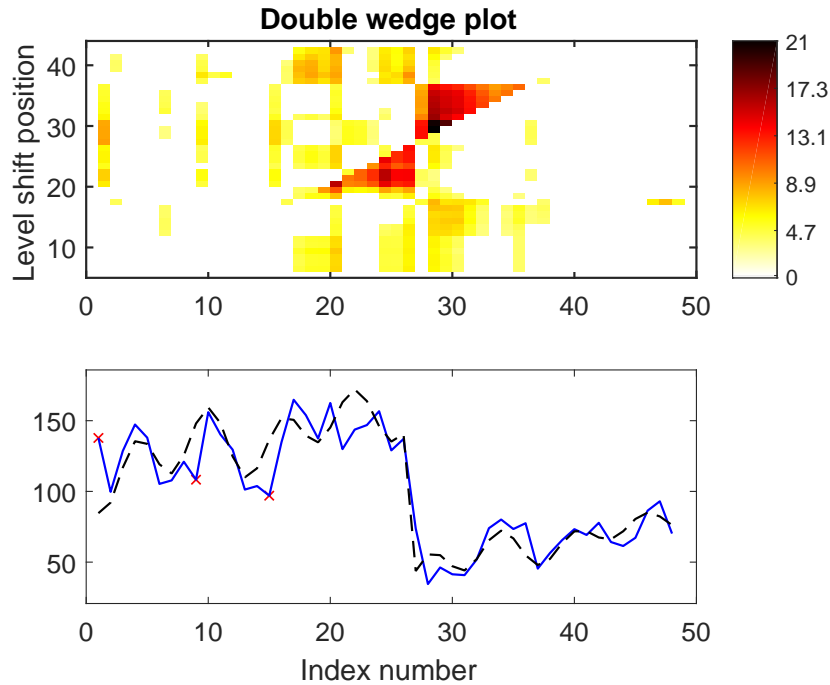


Figure 7: P12119085_KE_GB: double wedge plot (top) and observed and fitted values (bottom).

The robust fit to series P12119085-KE-GB (bottom panel of Figure 7) suggests three moderate outliers in positions 1, 9 and 15. The fit closely matches the level shift which is therefore well captured. The double wedge plot in the top panel of Figure 7 has two wedges which point to a level shift position around 27-28. The local refinement step selects position $t = 27$.

Columns 2–4 of Table 1 show the coefficients of the final fit together with their t -statistics and p -values. Most coefficients are significant, and in particular the t -statistic of the height of the level shift is quite large with $|t| = 14.7$. This drop looks anomalous because

in the period considered, Kenya was the only country of the East African Community (EAC) paying high European import duties on flowers and related products including CN 12119085. On the other hand, Kenya is the third largest exporter of cut flowers in the world. One would therefore check for a simultaneous upward level shift in an EAC country not paying import duties, which could point to a misdeclaration of origin.

Table 1: Coefficient estimates, t -statistics and p -values for series P12119085_KE_GB (columns 2-4) and P17049075_UA_LT (columns 5-7).

	P12119085_KE_GB			P17049075_UA_LT		
	Coeff	t -stat	p -values	Coeff	t -stat	p -values
$\hat{\alpha}_0$	115.27	25.6	0	55.14	14.3	0
$\hat{\alpha}_1$	1.59	5.80	0	0.90	4.52	0
$\hat{\beta}_{11}$	-2.83	-0.72	0.47	15.55	3.75	0.00056
$\hat{\beta}_{12}$	-12.42	-2.65	0.012	3.61	0.85	0.40
$\hat{\beta}_{21}$	-9.07	-1.95	0.059	-32.50	-7.64	0
$\hat{\beta}_{22}$	-22.60	-4.80	0	-16.06	-3.72	0.00061
$\hat{\gamma}_1$	-0.016	-3.72	0.00061	-0.023	-12.1	0
$\hat{\delta}_1$	-112.62	-14.7	0	-79.41	-13.9	0

Figure 8 shows the results for the second series, P17049075_UA_LT. The double wedge plot indicates the presence of a level shift around position 35. The local refinement yields the position $t = 34$. Interestingly, there is a reddish line right before the level shift. This is due to an outlier in position 32 which gets a red cross in the bottom panel of the figure. The double wedge plot also reveals a yellow strip at positions 29 and 30, indicating two less extreme outliers. Finally, the plot also shows some small reddish areas that correspond to local irregularities, for instance observations 4, 5, 17 and 18 which are flagged as outliers in the bottom panel. Columns 5–7 of Table 1 list the coefficients of the final fit. Also here most coefficients are strongly significant.

In this case the level shift might point to a different type of violation. The market of sugar and high-sugar-content products, such as CN code 17049075, is very restricted and regulated. The EU applies country-specific quotas for these products, with lower import

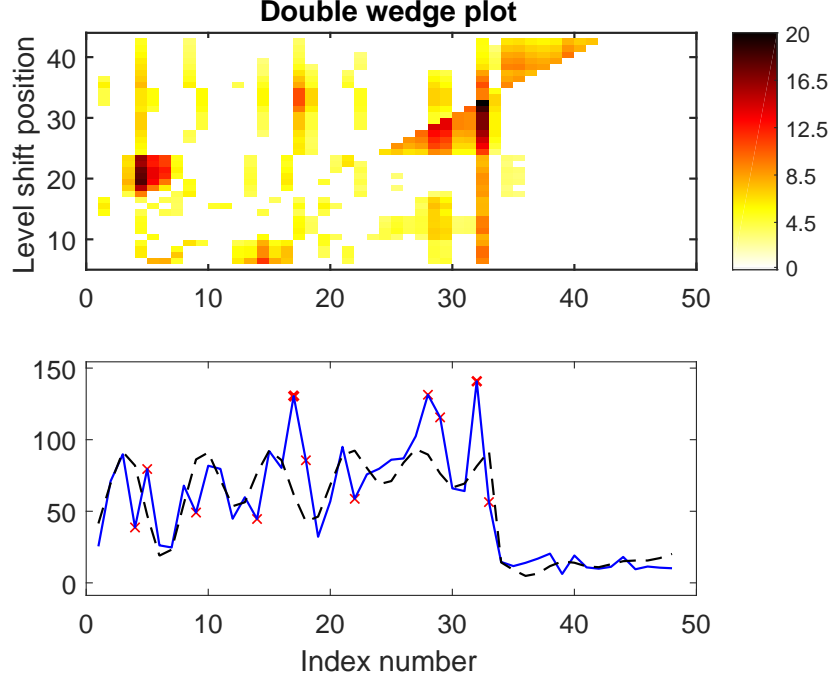


Figure 8: P17049075-UA_LT: double wedge plot (top) and observed and fitted values (bottom).

duty for imports below the quota and a higher duty beyond this limit (tariff rate quotas). Therefore, it would be in an exporter's interest to circumvent the quota by mislabeling this product as a somewhat related product that is not under surveillance. In this situation one would check for upward level shifts in related products from the same country.

We compared our results with those obtained by the nonparametric method introduced by Fried (2004) and Fried and Gather (2007) for robust filtering of time series. For this we used the function `robust.filter` from the R package `robfilter` of Fried et al. (2012). The robust fitting methods are applied to a moving time window of size `width`, which needs to be an odd number.

Tables 2 and 3 report the position of the level shift(s) and outlier(s) detected with all default options and various choices of window widths. We also tested different robust choices for the trend and scale estimation and some values for the `adapt` option which adapts the moving window width, with similar results.

Figures 9(a) and (b) show the resulting fits obtained by the nonparametric filter, for widths giving rise to the detection of a level shift (`width` = 7 for P_12119085_KE_GB and

Table 2: P_12119085_KE_GB: Positions of level shifts and outliers detected by a nonparametric time series filter, using different window widths.

Window width	Level shift position(s)	Outlier position(s)
3	-	[10, 16, 17, 37, 38, 46, 47]
5	-	[16, 17, 18, 47]
7	[27]	[17, 18]
9	[27, 37]	-
11	[27]	-

Table 3: P_17049075_UA_LT: Positions of level shifts and outliers detected by a nonparametric time series filter, using different window widths.

Window width	Level shift position(s)	Outlier position(s)
3	-	[2, 15, 44]
5	-	[15, 16, 17, 28, 30, 31, 33, 39, 40, 41]
7	-	[30, 31, 33, 34]
9	-	[30, 31, 33, 34, 35]
11	[30]	[32]

width = 11 for P_17049075_UA_LT). In the first series we see that the level shift is detected well for the appropriate width, but the fit itself is not as tight. Also in the second series a reasonable level shift position is found but the fit is not that close to the series. This can be explained by the fact that a nonparametric method has no prior knowledge about the data as it has to work on any data set, whereas our parametric model benefits from knowledge about the typical behavior of trade time series.

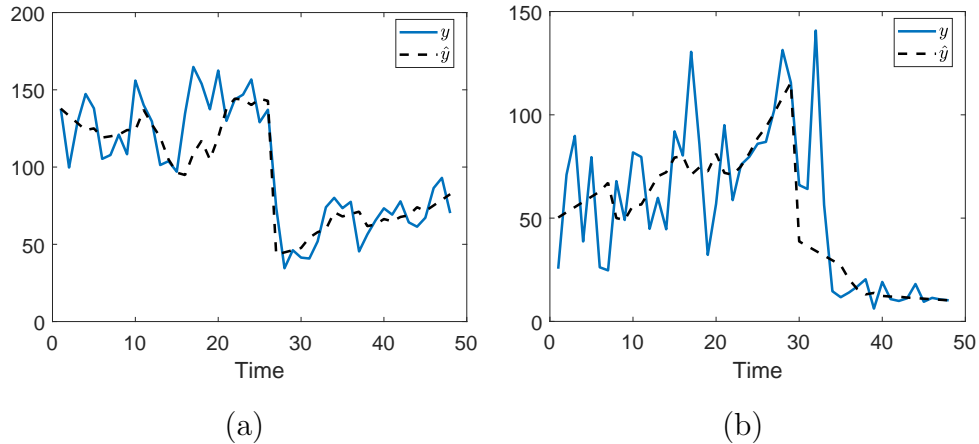


Figure 9: Fits obtained by a nonparametric time series filter for (a) P12119085_KE_GB; (b) P17049075_UA_LT.

5 Conclusions and outlook

We have introduced a new robust approach to model and monitor nonlinear time series with a possible level shift. A fast algorithm was developed and applied to several real and artificial datasets. We also proposed a new graphical display, the double wedge plot, which visualizes the possible presence of a level shift as well as outliers. This graph requires no additional computation as it is an automatic by-product of the estimation. Our approach thus allows to automatically flag outlying measurements and to detect a level shift, which is important in fraud detection as these may be indications of unauthorized transactions. At the European Joint Research Centre, this methodology was validated by comparing its results to those of visual inspection of many trade series by subject-matter experts.

Our basic model only considered the situation where at most one level shift can occur, which is a reasonable assumption for short time series. When several level shifts can occur, one could still apply our approach to the full time series. If it detects a level shift, we can modify the time series by undoing the break, that is, subtract $\hat{\delta}_1$ from all y_t to the right of the level shift, after which the procedure can be repeated. Alternatively, the time series could be split in the parts before and after the break, after which each part can be analyzed separately. These and other strategies are interesting topics for future research.

Appendix

Here we prove that a C-step (as used in the first step of the NLTS algorithm) can only decrease the LTS objective function.

Let $H^{(k)}$ be the current h -subset with its corresponding nonlinear LS coefficients $\hat{\theta}^{(k)} = (\{\hat{\alpha}^{(k)}\}, \{\hat{\beta}^{(k)}\}, \{\hat{\gamma}^{(k)}\}, \hat{\delta}_1^{(k)}, \hat{\delta}_2)$ and objective function $L^{(k)} = \sum_{t \in H^{(k)}} r_{(t)}^2(\hat{\theta}^{(k)})$.

Now consider $H^{(k+1)}$, the h -subset which contains the h observations with smallest squared residual with respect to $\hat{\theta}^{(k)}$. Then by construction

$$\sum_{t \in H^{(k+1)}} r_{(t)}^2(\hat{\theta}^{(k)}) \leq \sum_{t \in H^{(k)}} r_{(t)}^2(\hat{\theta}^{(k)}) = L^{(k)}. \quad (9)$$

The ALS step A then yields $\hat{\theta}^{(k+0.5)} = (\{\hat{\alpha}^{(k+1)}\}, \{\hat{\beta}^{(k)}\}, \{\hat{\gamma}^{(k+1)}\}, \hat{\delta}_1^{(k+1)}, \hat{\delta}_2)$. Since it is the LS solution of the linear model (5),

$$\sum_{t \in H^{(k+1)}} r_{(t)}^2(\hat{\theta}^{(k+0.5)}) \leq \sum_{t \in H^{(k+1)}} r_{(t)}^2(\hat{\theta}^{(k)}). \quad (10)$$

Next, ALS step B yields $\hat{\theta}^{(k+1)} = (\{\hat{\alpha}^{(k+1)}\}, \{\hat{\beta}^{(k+1)}\}, \{\hat{\gamma}^{(k+1)}\}, \hat{\delta}_1^{(k+1)}, \hat{\delta}_2)$ with

$$L^{(k+1)} = \sum_{t \in H^{(k+1)}} r_{(t)}^2(\hat{\theta}^{(k+1)}) \leq \sum_{t \in H^{(k+1)}} r_{(t)}^2(\hat{\theta}^{(k+0.5)}). \quad (11)$$

Combining (9)-(11) yields

$$L^{(k+1)} \leq L^{(k)}$$

so the new h -subset $H^{(k+1)}$ has an objective function that is less than or equal to that of $H^{(k)}$. Note that the only way to obtain equality is if no coefficients have changed, in which case the iteration stops.

References

- Agostinelli, C., A. Leung, V. Yohai, and R. Zamar (2015). Robust estimation of multivariate location and scatter in the presence of cellwise and casewise contamination. *Test* 24, 441–461.
- Barabesi, L., A. Cerasa, D. Perrotta, and A. Cerioli (2016). Modelling international trade data with the Tweedie distribution for anti-fraud and policy support. *European Journal of Operational Research* 258, 1031–1043.

- Bianco, A. M., M. Garca Ben, E. J. Martnez, and V. J. Yohai (2001). Outlier detection in regression models with arima errors using robust estimates. *Journal of Forecasting* 20(8), 565–579.
- Box, G. E. P. and G. M. Jenkins (1976). *Time Series Analysis: Forecasting and Control*. San Francisco: Holden Day.
- Čížek, P. (2005). Least trimmed squares in nonlinear regression under dependence. *Journal of Statistical Planning and Inference* 136, 3967–3988.
- Čížek, P. (2008). General trimmed estimation: robust approach to nonlinear and limited dependent variable models. *Econometric Theory* 24(6), 1500–1529.
- Croux, C. and P. J. Rousseeuw (1992). A class of high-breakdown scale estimators based on subranges. *Communications in Statistics - Theory and Methods* 21, 1935–1951.
- Fried, R. (2004). Robust filtering of time series with trends. *Journal of Nonparametric Statistics* 16(3-4), 313–328.
- Fried, R. and U. Gather (2007). On rank tests for shift detection in time series. *Computational Statistics & Data Analysis* 52(1), 221–233.
- Fried, R., K. Schettlinger, and M. Borowski (2012). *Package ‘robfilter’*. CRAN. URL: <http://www.statistik.tu-dortmund.de/fried.html>.
- Galeano, P. and D. Peña (2013). Finding outliers and unexpected events in linear and nonlinear possible multivariate time series data. In C. Becker, R. Fried, and S. Kuhnt (Eds.), *Robustness and Complex Data Structures. Festschrift in Honour of Ursula Gather*, pp. 255–273. Springer.
- Gervini, D. and V. J. Yohai (2002). A class of robust and fully efficient regression estimators. *Annals of Statistics* 30, 583–616.
- Pison, G., S. Van Aelst, and G. Willems (2002). Small sample corrections for LTS and MCD. *Metrika* 55, 111–123.

- Rousseeuw, P. (1984). Least median of squares regression. *Journal of the American Statistical Association* 79, 871–880.
- Rousseeuw, P. and K. Van Driessen (2006). Computing LTS regression for large data sets. *Data Mining and Knowledge Discovery* 12, 29–45.
- Salini, S., A. Cerioli, F. Laurini, and M. Riani (2015). Reliable robust regression diagnostics. *International Statistical Review* 84, 99–127.
- Stromberg, A. (1993). Computation of high breakdown nonlinear regression parameters. *Journal of the American Statistical Association* 88, 237–244.
- Stromberg, A. and D. Ruppert (1992). Breakdown in nonlinear regression. *Journal of the American Statistical Association* 87, 991–997.